A Network Modeling Approach to Analysis of the Th2 Memory Responses Underlying Human Atopic Disease[1]

Anthony Bosco, Kathy L. McKenna, Martin J. Firth, Peter D. Sly, and Patrick G. Holt[2]

Complex cellular functions within immunoinflammatory cascades are conducted by networks of interacting genes. In this study, we employed a network modeling approach to dissect and interpret global gene expression patterns in allergen-induced Th cell responses that underpin human atopic disease. We demonstrate that a subnet of interconnected genes enriched for Th2 and regulatory T cell-associated signatures plus many novel genes is hardwired into the atopic response and is a hallmark of atopy at the systems level. We show that activation of this subnet is stabilized via hyperconnected "hub" genes, the selective disruption of which can collapse the entire network in a comprehensive fashion. Finally, we investigated gene expression in different Th cell subsets and show that regulatory T cell- and Th2-associated signatures partition at different stages of Th memory cell differentiation. Moreover, we demonstrate the parallel presence of a core element of the Th2-associated gene signature in bystander naive cells, which can be reproduced by rIL-4. These findings indicate that network analysis provides significant additional insight into atopic mechanisms beyond that achievable with conventional microarray analyses, predicting functional interactions between novel genes and previously recognized members of the allergic cascade. This approach provides novel opportunities for design of therapeutic strategies that target entire networks of genes rather than individual effector molecules. *The Journal of Immunology,* **2009, 182: 6011–6021.**

The general concept that complex immunological diseases such as atopy are driven via integrated pathways or molecular cascades has been accepted dogma for more than two decades. The approaches to identification of relevant cascade members and in particular those that are rate limiting in the disease process driven by the cascade have not evolved greatly over this period, and they generally focus on candidate effector or regulator molecules selected stepwise on the basis of their known effector functions and their potential interactions with other perceived pathogenic factors. However, the level of clinical efficacy achieved with therapies designed to target simple linear pathways or causal chains has been disappointing (1, 2).

The development of global gene expression profiling technologies has provided opportunities for new approaches to the same problem. The conceptual leap of principal interest in this context comes from the way in which these data are analyzed, in particular the emergence of quantitative algorithms based on network theory (3). This new approach enables a systems-level characterization of the networks of interacting genes that underpin cellular function and behavior, unearthing pathways at the core of disease processes.

A fundamental organizing principle of gene networks is their scale-free topology, meaning that network connectivity is dominated by a few centralized genes designated "hubs", which are hyperconnected to a larger number of peripheral genes with few connections (3). This structural feature of gene networks, coupled with additional mechanisms including feedback control, redundant wiring, and plasticity, is thought to bestow biological systems with a high degree of tolerance to perturbations such as gene deletions (4–8). However, a scale-free organization has an inherent trade-off, because removal of hyperconnected hubs at any level of biological organization (DNA, mRNA, protein, metabolite) can result in severe or multiple phenotypes (8–14).

By inference, entire networks of immunological disease-associated genes relevant to activation of Th memory responses may also be under the control of hubs; however, this remains to be formally demonstrated, because the tools of network analysis have not yet been systematically applied broadly in the immunology field (15). In the study herein, we have utilized these methodologies to reanalyze the $CD4^+$ Th memory responses that underpin human atopic disease, in particular responses to house dust mite (HDM)[3] allergen, which is a major trigger of atopic asthma. We focus on the early activation phase in HDM-triggered Th memory cells isolated from blood to minimize distortion of the gene expression program that may result from in vitro manipulations (16). We demonstrate that gene coexpression network analysis predicts functional associations between novel and known genes and provides an additional level of insight into the operation and stabilization of the principal atopy-associated effector pathway.

Materials and Methods

Study population

The study population included healthy volunteers comprising HDM-sensitized atopics and nonatopic controls in the age range 14–45 years. Atopic status to HDM was defined by positive skin test reaction to

Telethon Institute for Child Health Research, and Centre for Child Health Research, Faculty of Medicine and Dentistry, The University of Western Australia, Perth, Western Australia, Australia

Received for publication December 10, 2008. Accepted for publication March 10, 2009.

The costs of publication of this article were defrayed in part by the payment of page charges. This article must therefore be hereby marked *advertisement* in accordance with 18 U.S.C. Section 1734 solely to indicate this fact.

[1] This work was supported by the National Health & Medical Research Council of Australia and National Institutes of Health Grant 1R21AI78511-1.

[2] Address correspondence and reprint requests to Dr. Patrick G. Holt, Division of Cell Biology, Telethon Institute for Child Health Research, PO Box 855, West Perth, Western Australia 6872, Australia. E-mail address: patrick@ichr.uwa.edu.au; anthonyb@ichr.uwa.edu.au

[3] Abbreviations used in this paper: HDM, house dust mite; FDR, false discovery rate; qRT-PCR, quantitative real-time RT-PCR; SAM, significance analysis of microarray; T_{CM}, central memory Th cell; T_{EM}, effector memory Th cell; T_N, naive Th cell; T_{TM}, transitory memory Th cell; Treg, regulatory T cell.

www.jimmunol.org/cgi/doi/10.4049/jimmunol.0804125

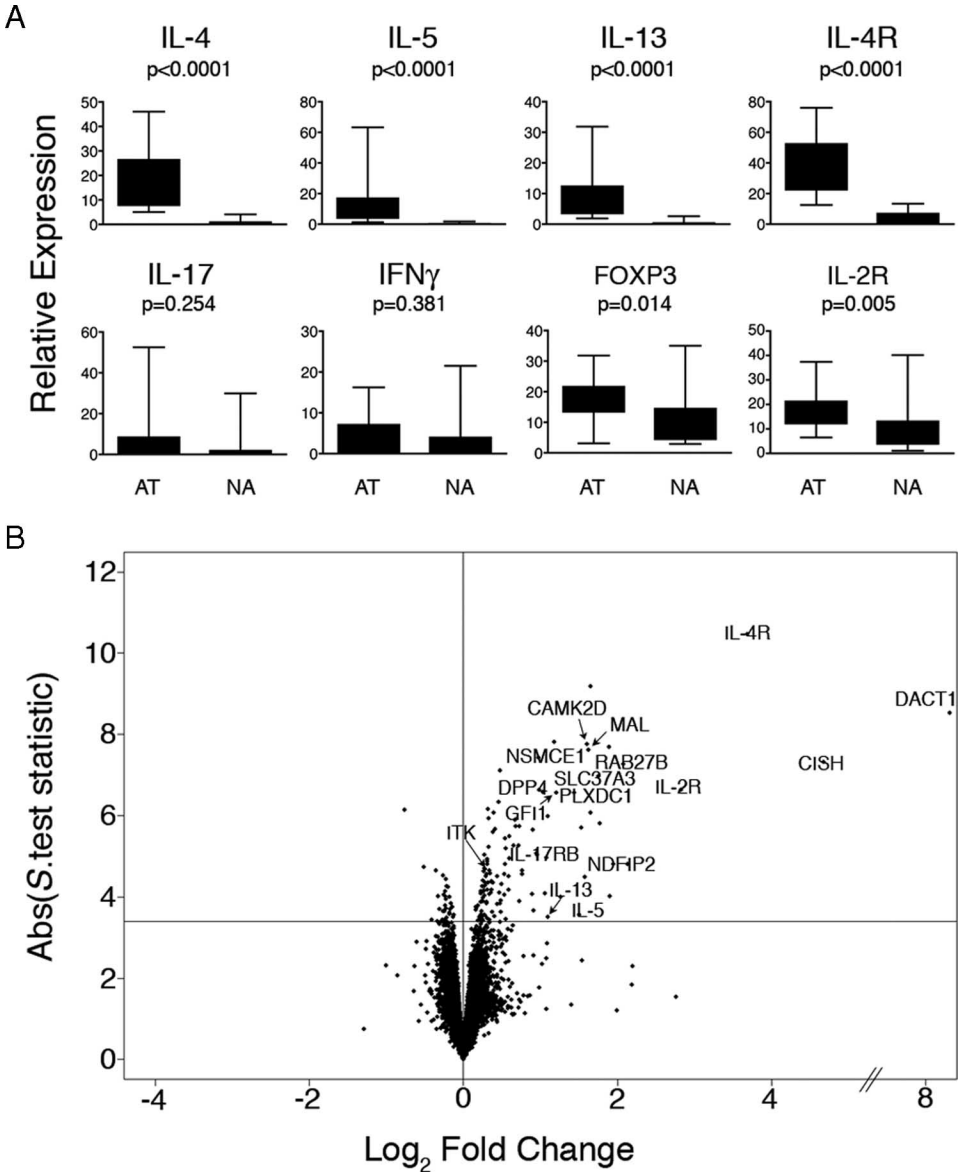

FIGURE 1. $CD4^+$ Th cell response patterns to allergens in atopic and nonatopic subjects. PBMC from HDM-sensitized atopics ($n = 15$) and nonatopic controls ($n = 15$) were cultured in the presence or absence of HDM for 24 h. At the termination of the cultures, $CD4^+$ Th cells were isolated and gene expression was profiled by qRT-PCR and microarray analysis. *A*, qRT-PCR analysis of selected Th lineage signature genes demonstrates the Th2-skewed response phenotype of the atopic subjects. Data are expressed as gene expression level above baseline relative to the stably expressed gene EEF1A1 (68). AT, Atopic; NA, nonatopic. Statistical analysis by Mann-Whitney *U* test. *B*, Microarray analysis of differential gene expression in atopic and nonatopic responses. Background-corrected gene expression levels (level in HDM-stimulated cells relative to baseline control (HDM/control)) were compared in atopic and nonatopic responses employing the *S* test (20). The data are summarized as a volcano plot (21), which displays microarray data along axes of statistical significance (absolute *S* test statistic) and differential expression magnitude (atopic HDM/control:nonatopic HDM/control on the $\log_2$ scale ($\log_2$ fold change)). Genes above the horizontal line are significantly differentially expressed (FDR adjusted *p* value <0.01); positive and negative values on the horizontal axis indicate elevated expression in atopic and nonatopic responses, respectively. ABS, absolute.

HDM extract (wheal ≥3 mm) and the presence of HDM-specific serum IgE (≥0.7 kU/L). The study was approved by our institutional human ethics committee.

Cell preparation and culture methodologies

PBMC were thawed from cyrobanked samples and cultured in AIM-V medium (Invitrogen) in the presence or absence of 10 μg/ml HDM extract (*Dermatophagoides pteronyssinus*; CSL) for 24 h as detailed previously (17). At the termination of the cultures, $CD8^+$ followed by $CD4^+$ T cells were isolated by positive selection employing immunomagnetic separation (Dynal Biotech). The purity of the $CD4^+$ T cells was not tested in every sample but was routinely 98.1% (±0.1%). Where specified, 1 U/ml human recombinant IL-2 (Cetus), 0.25 ng/ml human recombinant IL-4 (ProSpec-Tany TechnoGene), 5 mg/ml anti-IL-2 (clone MQ1-17H12; BD Pharmingen), or 5 mg/ml anti-IL-4 (clone MP4-25D2; BD Pharmingen) was added to the cultures. Replicate cultures containing appropriate isotype control Abs (clones R35-95 and R3-34; BD PharMingen) were set up in parallel.

For cell sorting experiments, PBMC were labeled with anti-CD27-FITC, anti-CD45RA-PE-Cy5, anti-CD3-allophycocyanin-Cy7, anti-CD4-allophycocyanin (BD Biosciences), and anti-CCR7-PE (R&D Systems) and sorted on a FACSAria (BD Biosciences). Postsort purities of the CD4 subpopulations (T_N, T_{CM}, T_{EM}) ranged from 95% to 99%, except for the T_{TM} subset, which ranged in purity from 80% to 97% (mean, 89%).

Quantitative real-time RT-PCR (qRT-PCR) analysis

Total RNA samples were extracted employing TRIzol (Invitrogen) followed by RNeasy (Qiagen). The quality of the RNA was not tested in every sample, but the RNA integrity number was routinely 8.8 (±0.03) as assessed on the Bioanalyzer (Agilent). Reverse transcription was performed with the Omniscript kit (Qiagen), and qRT-PCR was performed with QuantiTect SYBR Green (Qiagen) employing predeveloped assays (Qiagen) as described previously (16). Where specified, qRT-PCR data were log transformed, mean centered, and scaled (see *Statistical analysis*).

Microarray study design

A total of 90 microarrays were employed in the study to profile gene expression in paired samples of HDM-stimulated and unstimulated $CD4^+$ T cells from 45 subjects. The experimental design comprised two independent atopic data sets ($n = 15$ subjects in each set) for network construction and validation, and a nonatopic data set ($n = 15$) for statistical comparisons.

Microarray methodologies and data preprocessing

Total RNA (~100 ng) from $CD4^+$ T cells was labeled and hybridized to Human Gene 1.0 ST microarrays (Affymetrix), employing standardized protocols and reagents from Affymetrix. The microarray data were preprocessed in Expression Console software (Affymetrix) employing the probe logarithmic intensity error algorithm (PLIER, parameters: PM-GCBG

background subtraction, quantile normalization, iterPLIER summarization). The preprocessed microarray data were then imported into the R language and environment for statistical computing (www.r-project.org/) for further analysis. Variance stabilization was performed by adding the small constant 16 to all the data points, followed by $\log_2$ transformation. The microarray data are available in the Gene Expression Omnibus repository (www.ncbi.nlm.nih.gov/projects/geo/) under the accession number GSE: 14908.

Identification of the atopy transcriptome in human CD4$^+$ Th cell responses

The moderated *t* test (18) was employed to identify genes that were significantly modulated in allergen-stimulated vs unstimulated cells from atopic (atopic transcriptome) and nonatopic (nonatopic transcriptome) subjects. The moderated *t* test employs a Bayesian model to leverage information obtained from the variability across all the genes to make inferences about individual genes. To account for multiple testing, the *p* values derived from the moderated *t* test statistics were adjusted employing the false discovery rate (FDR) method (19). Only genes that were significantly (FDR-adjusted *p* value <0.01) modulated by $\geq$1.2-fold after HDM stimulation were considered in further analyses.

Differential expression analysis of CD4$^+$ Th cell response patterns to allergens

To identify differences in the response profiles of atopic and nonatopic subjects, background corrected gene expression levels (i.e., level in HDM-stimulated cells relative to baseline control (HDM/control) on the $\log_2$ scale) for the HDM-regulated genes identified above (i.e., the combined atopic and nonatopic transcriptomes) were analyzed employing the significance analysis of microarrays test (SAM or *S* test) (20). The *S* test is a variant of the *t* test, which adds a small constant to the variability component of the gene-specific *t* test. Differentially expressed genes are identified by comparing the *S* test statistics with their null distribution, which is generated via permutation of the sample class labels. The significance level of a SAM analysis is dependent on the tuning parameter δ, and for each value of δ, the FDR is calculated as the 90th percentile of the number of false-positive genes divided by the number of genes called significant. A value for δ was selected corresponding to a 90th percentile FDR of <0.01. The results of the *S* test analysis were summarized on a volcano plot (21), a scatter plot of the *S* test statistics vs the $\log_2$ fold change (atopic HDM/control:nonatopic HDM/control).

Gene coexpression network analysis

Network analysis was performed on the microarray data employing the weighted gene coexpression algorithm developed by Horvath and coworkers (10). The mathematical process involves calculating absolute Pearson correlations for all pairwise gene-gene combinations across the test samples. The correlations were transformed into connection strengths by raising them to a power β. The value for β was selected by fitting a statistical model to the data, which is based on the knowledge that the distribution of connectivity in biological networks follows a scale-free topology (10). Genes with a low connectivity to the network were removed from the analysis (bottom 20% with low values for k_{total}, see below). To identify modules of interconnected genes, the topological overlap was calculated from the pairwise connection strengths and analyzed by hierarchical clustering (10, 22). The topological overlap is a measure of the degree in which each pair of genes is correlated with the same set of genes. The modules were defined from the dendrogram output of the hierarchical clustering analysis employing an automated adaptive algorithm (23).

To test individual modules for association with atopic status, background-corrected gene expression levels (HDM/control on $\log_2$ scale) in atopic vs nonatopic responses were compared on a module-by-module basis employing gene set analysis (24). Gene set analysis tests for the association of a set of genes rather than individual genes with a phenotype of interest, and it employs randomization/resampling of the genes to avoid bias in the determination of the test statistic, as well as permutations of the samples to estimate the FDR and account for correlations between genes (24). To illustrate module enrichment, background-corrected gene expression levels (HDM/control) in atopic vs nonatopic responses were compared employing the *S* test (20), and the absolute value of the *S* test statistics were plotted as box-and-whisker plots on a module-by-module basis.

The interaction of each component gene to the other genes in the network is quantified by the connectivity (*k*). The connectivity of a gene is defined as the cumulative connectivity (i.e., sum of the pairwise connection strengths) and can be calculated with respect to the entire network (K_{total}) or within a specific module (K_{in}). The K_{in} values were scaled to lie between 0 and 1.

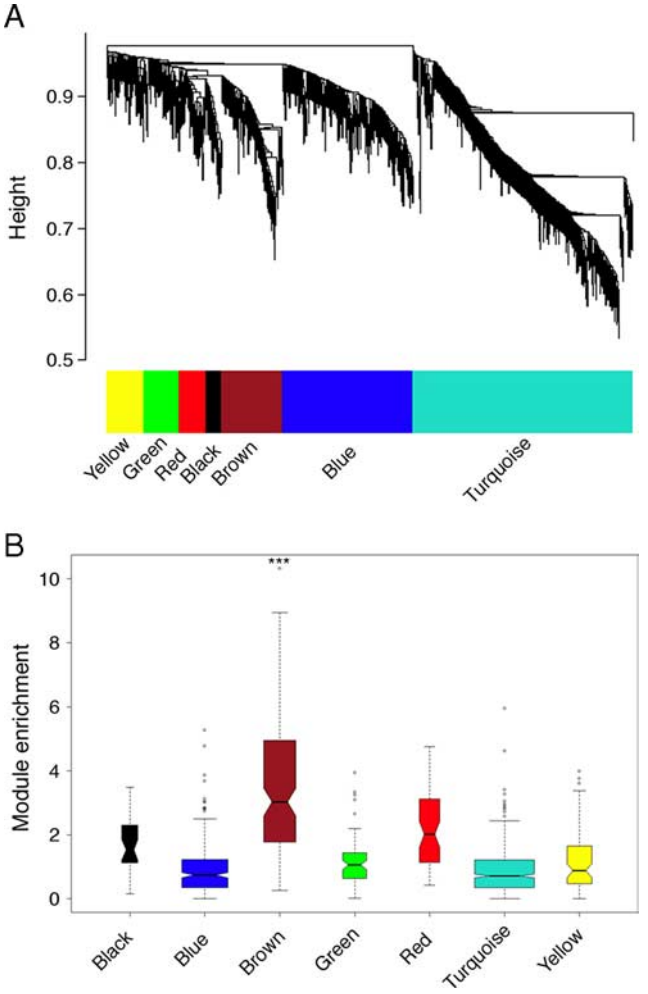

FIGURE 2. Modular architecture of the gene coexpression network in atopic CD4$^+$ Th cell responses to allergens; variations associated with allergic sensitization. *A*, Network analysis was performed on the atopic CD4$^+$ Th cell response microarray data set from Fig. 1*B*, and hierarchical clustering was employed to resolve the network into subnets (modules) of highly interconnected genes (10). The modules were defined by an automated algorithm (23) and can be visualized as the internal branch-like structures of the dendrogram output from the cluster analysis. *B*, The brown module is uniquely associated with atopic status. Background-corrected gene expression levels (HDM/control) were compared in atopic and nonatopic responses employing the *S* test (20), and the absolute value of the *S* test statistics were graphed as box-and-whisker plots on a module-by-module basis to visualize module enrichment. Statistical analyses were performed to compare the overall expression of each module in atopic and nonatopic responses employing gene set analysis (***, FDR-adjusted *p* value <0.001) (24).

Statistical analyses

The statistical methods used in this study were performed in the R environment including the moderated *t* test (18), *S* test (20), gene set analysis (24), gene coexpression network analysis (10), Wilcoxon signed-rank test, Mann-Whitney *U* test, paired *t* test, Spearman's rank correlation, Fisher's exact test, and hierarchical clustering (10). Where specified, FDR-adjusted *p* values (19) were reported to control for type I error when performing multiple hypothesis testing. Gene set analysis and the *S* test have built-in functions based on data resampling techniques to calculate the FDR; for all other statistical methods, the FDR was calculated employing the Benjamini and Hochberg method (19) in the R package multtest (available at www.bioconductor.org/). It is noteworthy that the Benjamini and Hochberg FDR

Table I. *Functional annotation of the consensus atopy module*[a]

Function/Pathway	Gene Symbol	Chromosome	Gene Name
Apoptosis	BCL2	18q21.33	B cell CLL/lymphoma 2
	BTG1[b]	12q22	B cell translocation gene 1
	CASP3	4q34	Caspase 3
	STK17B	2q32.3	Serine/threonine kinase 17b; DRAK2
Inflammation and immunoregulation	CD200R1	3q13.2	CD200 receptor 1
	CISH	3p21.3	Cytokine inducible SH2-containing protein
	CSF1	1p21–p13	CSF1
	IL-1F6[b,c]	2q12–q14.1	IL-1 family, member 6 (ϵ)
	LIF	22q12.2	Leukemia inhibitory factor
	SOCS2	12q	Suppressor of cytokine signaling 2
Leukotriene and prostaglandin signaling	ALOX5	10q11.2	Arachidonate 5-lipoxygenase
	HPGD	4q34–q35	Hydroxyprostaglandin dehydrogenase
	PTGER2	14q22	Prostaglandin E receptor 2 (EP2 receptor)
Protease activity and regulation	PITRM1[b]	10p15.2	Pitrilysin metallopeptidase 1
	SPINT2	19q13.1	Serine peptidase inhibitor, Kunitz type, 2
	TPP2[b,c]	13q32–q33	Tripeptidyl peptidase II
Protein trafficking	RAB19B[b]	7q34	GTP-binding protein RAB19B (RAB19)
	RAB27B	18q21.2	RAB27B, member RAS oncogene family
	RAB30	11q12–q14	RAB30, member RAS oncogene family
Signal transduction	ARRDC2[b,c]	19p13.11	Arrestin domain containing 2
	CNKSR2[b]	Xp22.12	Connector enhancer of kinase suppressor of Ras 2
	KPNA6[b]	1p35.1–p34.3	Karyopherin α6 (importin α7)
	NCOA3	20q12	Nuclear receptor coactivator 3
	NDFIP2	13q31.1	Nedd4 family-interacting protein 2
	NSMCE1	16p12.1	Non-SMC element 1 homolog
	PGM1[b]	1p31	Phosphoglucomutase 1
	RAP2B[c]	3q25.2	RAP2B, member of RAS oncogene family
	RASL11A[b]	13q12.2	RAS-like, family 11, member A
	SOCS2	12q	Suppressor of cytokine signaling 2
	TBC1D1[b]	4p14	TBC1 domain family, member 1
Solute carrier activity	SLC26A11[b]	17q25.3	Solute carrier family 26, member 11
	SLC37A3	7q34	Solute carrier family 37, member 3
	SLC39A8	4q22–q24	Solute carrier family 39, member 8
TcR signaling	APBB1IP[b,c]	19p13.11	Rap1-interacting adaptor molecule (RIAM)
	CEACAM1	19q13.2	Carcinoembryonic Ag-related cell adhesion 1
	CISH	3p21.3	Cytokine inducible SH2-containing protein
	DPP4	2q24.3	Dipeptidyl-peptidase 4 (CD26)
	IL-2R	10p15–p14	IL-2 receptor, α
	ITK	5q31–q32	IL-2-inducible T cell kinase
	LCP2[c]	5q33.1-qter	Lymphocyte cytosolic protein 2 (SLP-76)
	MAL	2cen–q13	Mal, T cell differentiation protein
	RAP1A	1p13.3	RAP1A, member of RAS oncogene family
Th2 regulation and function	CCL1	17q12	C-C chemokine ligand 1, I-309
	GFI1	1p22	Growth factor independent 1
	ID2	2p25	Inhibitor of DNA binding 2
	IL-13	5q31	IL-13
	IL-17RB	3p21.1	IL-17 receptor B (IL-25 receptor)
	IL-4R	16p11.2–12.1	IL-4 receptor
	IL-5	5q31.1	IL-5
	ITK	5q31–q32	IL-2-inducible T cell kinase
	RRS1[c]	8q13.1	RRS1 ribosome biogenesis regulator homolog
Treg expression and function	CISH	3p21.3	Cytokine inducible SH2-containing protein
	FOXP3	Xp11.23	Forkhead box P3
	GFI1	1p22	Growth factor independent 1
	HIPK2	7q32–q34	Homeodomain-interacting protein kinase 2
	IKZF4[b,c]	12q13	IKAROS family zinc finger 4 (Eos)
	IL-2R	10p15–p14	IL-2 receptor, α
	ITK	5q31–q32	IL2-inducible T cell kinase
	PTGER2	14q22	Prostaglandin E receptor 2 (EP2 receptor)
	SOCS2	12q	Suppressor of cytokine signaling 2
	TIAM1[b]	21q22.1	T-cell lymphoma invasion and metastasis 1
Transcriptional regulation	BATF[b,c]	14q24.3	Basic leucine zipper transcription factor, ATF-like
	ENO1[b,c]	1p36.3–p36.2	Enolase 1 (α)
	HIPK1[b]	1p13.2	Homeodomain-interacting protein kinase 1
	ID2	2p25	Inhibitor of DNA binding 2
	IKZF1[c]	7p13–p11.1	IKAROS family zinc finger 1 (Ikaros)
	IKZF4[b,c]	12q13	IKAROS family zinc finger 4 (Eos)
	KLF3[c]	4p14	Krüppel-like factor 3 (basic)
	LASS6[b]	2q24.3	LAG1 homolog, ceramide synthase 6
	PCGF5[c]	10q23.32	Polycomb group ring finger 5
	TSC22D3[c]	Xq22.3	TSC22 domain family, member 3; GILZ

(*Table continues*)

Table I. (*Continued*)

Function/Pathway	Gene Symbol	Chromosome	Gene Name
Wnt/β-catenin signaling	BCL9L[b,c]	11q23.3	Bcell CLL/lymphoma 9-like
	CAMK2D	4q26	Calcium-dependent protein kinase II δ
	DACT1	14q23.1	Dapper homolog 1
	HIPK2	7q32–q34	Homeodomain-interacting protein kinase 2
	ID2	2p25	Inhibitor of DNA binding 2
	MEOX1[b]	17q21	Mesenchyme homeobox 1
	TIAM1[b]	21q22.1	T cell lymphoma invasion and metastasis 1
Unclassified or unknown function	ETNK1[b]	12p12.1	Ethanolamine kinase 1
	FAM102B[b]	1p13.3	Family with sequence similarity 102, member B
	GNPDA1[b]	5q21	Glucosamine-6-phosphate deaminase 1
	IMMT	2p11.2	Inner membrane protein, mitochondrial (mitofilin)
	OBFC2A[b]	2q32.3	Oligonucleotide-binding fold containing 2A
	PLXDC1	17q21.1	Plexin domain containing 1
	SNTB1	8q23–q24	Syntrophin, β1

[a] Genes were assigned to functional classes (some genes in more than one class) based on classifications from the Gene Ontology consortium (www.geneontology.org/), as well as manual curation based on information from the literature and other sources. See supplemental Table S2 for additional information and references.

[b] Novel genes that have not been previously reported in the context of atopy or Th2 regulation.

[c] Genes that were specifically detected as atopy-associated based on their patterns of interconnectivity with other members of the atopy module, but were not detected as atopy-associated by differential expression analyses in Fig. 1*B*.

procedure is appropriate for test statistics that are independent or positively correlated (25).

Before statistical analysis employing the *t* test, qRT-PCR data points below the detection limit (DL) were substituted for DL/2 followed by $\log_{10}$ transformation to correct for data skewness and heteroscedasticity (26).

Before hierarchical clustering analysis, mean centering and unit variance scaling was performed on the qRT-PCR data to emphasize the more relevant variations between samples as opposed to differences in high or low abundance values (26).

Results

Identification of the atopy transcriptome in human CD4$^+$ Th cell responses

To characterize the patterns of gene expression in Th cell responses to allergens, PBMC from panels of HDM-sensitized atopics ($n = 15$) and nonsensitized nonatopic controls ($n = 15$) were cultured in the presence or absence of HDM allergens for 24 h. At the termination of the cultures, CD4$^+$ Th cells were isolated by immunomagnetic separation, and gene expression was analyzed by qRT-PCR. As illustrated in Fig. 1*A*, the atopic Th cell response phenotype was Th2-skewed, as predicted from previous studies employing this culture system (16, 17). Regulatory T cell (Treg) signature genes (IL-2R, FoxP3) were also elevated in the atopic responses; however, it is noteworthy that these genes are also transiently up-regulated following the activation of conventional Th cells (reviewed in Ref. 27).

Microarray profiling was then performed to investigate changes in global patterns of gene expression. Paired comparisons of HDM-stimulated Th cells with unstimulated Th cells demonstrated that a substantial gene expression program was activated in the respective responses, comprising 1442 genes in the atopic responses (i.e., the atopy transcriptome) and 1243 genes in the controls (average fold change >1.2 and FDR (19) adjusted *p* value <0.01; moderated *t* test (18)). Consistent with our previous findings, many of these genes were common to both groups (16); however, ~150 genes differed between the respective responses after accounting for multiple testing (FDR-adjusted *p* value <0.01; significance analysis of microarray *t* test (20); supplemental Table S1).[4] As illustrated in Fig. 1*B*, most of these genes were elevated in the atopic responses, including several previously recognized members of the Th2 cascade (IL-4R, IL-5, IL-13, GFI-1, ITK), as well as a cohort of novel Th2-associated genes (IL-17RB, CAMK2D, CISH, DACT1, DPP4, MAL, NDFIP2, NSMCE1, PLXDC1) reported recently by us (16) and confirmed in an independent study (28).

Characterization of the coexpression network architecture of the atopy transcriptome in CD4$^+$ Th cell responses

The statistical analyses performed above identify a list of genes involved in Th memory responses to allergens, but they provide limited insight into how these genes interact to control the underlying T cell activation process. To obtain more detailed information in this regard, a systems-level analysis was performed on the atopic data set, employing a weighted gene coexpression network reconstruction algorithm as detailed in *Materials and Methods* (10). Briefly, network analysis employs a stepwise analytical process to leverage variations in gene-by-gene correlations across the samples to describe in quantifiable terms the underlying gene networks. Pathways manifest as subnets of highly correlated genes ("modules"), and hyperconnected genes ("hubs") are identified within pathways. The algorithm generates a branching tree-like diagram output (dendrogram), in which modules of highly correlated genes are identified as the internal branch-like structures of the dendrogram. As illustrated in Fig. 2*A*, network analysis resolved the atopy transcriptome into a gene coexpression network composed of a series of seven discrete modules. Of note, the distribution of connectivity followed a scale-free topology (data not shown), as predicted from studies in other systems (3, 29). To determine whether any of the modules were associated with atopy, we performed a statistical comparison of the overall expression of each module in the atopic and nonatopic responses. As illustrated in Fig. 2*B*, the results demonstrated that one of the modules was uniquely associated with atopic status (module-level FDR adjusted *p* value <0.001 by gene set analysis (24)).

To determine whether the atopy-associated module is reproducible, an additional series of microarray profiles was generated from HDM-stimulated CD4$^+$ Th cells from an independent panel of atopics ($n = 15$). Network analysis of this independent data set revealed a similar coexpression network comprising discrete modules (not shown), and again a striking association was observed between a single module and atopic status (module-level FDR adjusted *p* value <0.001 by gene set analysis (24)). The overlap between these two putative atopy-associated modules comprising 71 genes was highly significant (Fisher's exact test *p* value $< 1 \times 10^{-15}$) and included signatures associated with the activation of

[4] The online version of this article contains supplemental material.

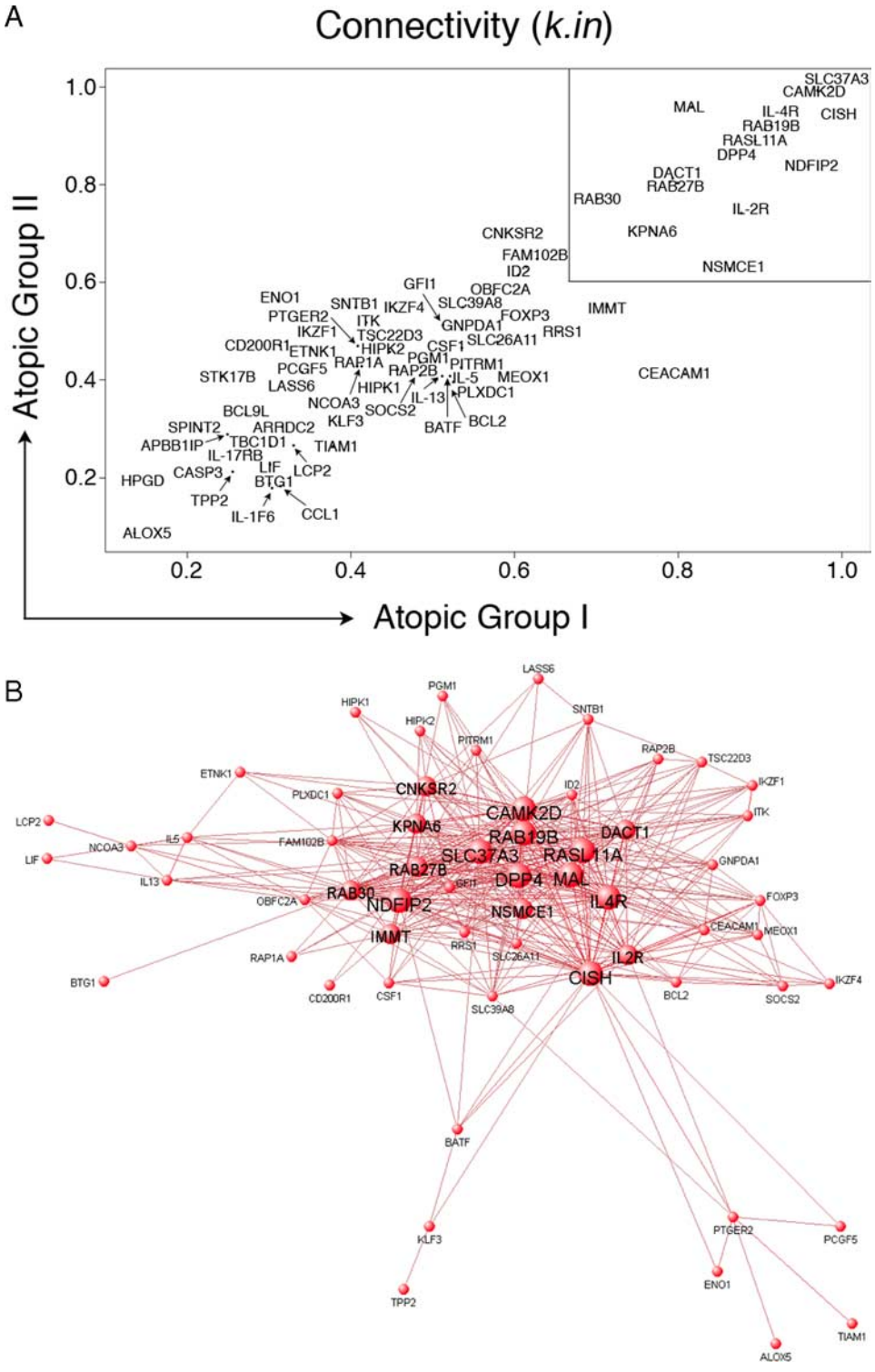

FIGURE 3. Visualization of the atopy-associated module and identification of putative hubs. *A*, Network analysis was performed separately on the two independent atopic CD4$^+$ Th cell response microarray data sets, and variations in the patterns of connectivity within the atopy module were investigated by calculating the k_{in} (see *Materials and Methods*). Hyperconnected hub genes have a k_{in} approaching 1.0 and are therefore located in the upper right region of the scatter diagram (box). The k_{in} values were highly correlated across the two independent data sets (Spearman rho = 0.84, p value $<1 \times 10^{-15}$). *B*, A graphical representation of the atopy-associated module. The microarray data from the two independent atopic data sets were pooled and network analysis was performed. The top gene-gene interaction data (i.e., all pairwise connection strengths >0.25; corresponding to the top ~500 interactions) within the module were submitted to VisANT software (visant.bu.edu/) for network visualization. To illustrate the hubs, progressively larger font and node sizes were selected based on the connectivity data, which was partitioned into four categorical bins of >31 links, 21–30 links, 11–20 links, and <10 links. The hubs appear as the large central nodes in the network diagram.

Th2 cells (IL-4R, IL-5, IL-13, ITK, GFI-1, CAMK2D, CISH, DACT1, DPP4, MAL, NDFIP2, PLXDC1, PTGER2, RAB27B) and Tregs (CISH, FoxP3, GFI-1, HIPK2, ID2, IKZF4, ITK, IL-2R, PTGER2, SOCS2, TIAM1 (30)), as well as a range of novel genes (Table I; see supplemental Table S2 for references). This overlapping gene set was designated the "consensus atopy module", and accordingly became the principal focus of the remainder of this study. Of note, 15 out of the 71 genes in the atopy module were not detected by the conventional statistical analyses performed above (Fig. 1*B*), even when the FDR threshold was reduced from 0.01 to 0.05, suggesting that network analysis can unmask cryptic variations in gene expression, thus revealing covert disease-associated genes (Table I).

The consensus atopy-associated module is enriched with functionally coherent genes

Modules execute high level biological functions by mobilizing sets of coexpressed genes that function in the same pathway (29, 31). As detailed in Table I, the atopy-associated module was enriched for functionally coherent genes involved in TCR and Wnt/β-catenin signaling, signal transduction, transcriptional regulation, Th2 regulation and function, inflammation, and Treg function.

Although a generic function has been assigned to most of the genes in the module by the gene ontology consortium, for the vast majority of genes there is no information available about their regulation and/or function specifically in T cells. Moreover, the module contained 25 genes that have not previously been reported in the context of atopy (Table I).

Validation of constituent genes in the consensus atopy-associated module

Microarray detection of thousands of molecules in a single assay can result in false-positive signals due to nonspecific background and cross-hybridization (32). Therefore, we sought confirmation of expression of the module genes in atopic Th cell responses to allergens via more quantitative RT-PCR methodology, employing the RNA samples from the independent groups of study subjects used for the microarray experiments. At least 90% of the genes tested were validated in these analyses (supplemental Table S3), which incorporated FDR controls for multiple hypothesis testing (19).

Additional validation across microarray platforms was provided via metaanalysis of in-house data sets on mixed $CD4^+$ and $CD8^+$ atopic T cell responses to HDM, which were generated as reported earlier (16) on the previous series Affymetrix microarrays. These analyses identified a module that significantly overlapped with the consensus atopy module (Fisher's exact test p value of 5.5×10^{-7}). In addition to the core Th2 cluster on chromosome 5q31.1, these analyses also identified a broad range of the novel genes illustrated in Table I, including BATF, CAMK2D, CEACAM1, DACT1, NDFIP2 and RAB27B (data not shown).

Variations in connectivity within the atopy-associated module reveals hyperconnected hubs, which are essential for overall module functionality

Systematic studies in other systems have reported that the connectivity of individual genes within biological networks is correlated with essential functions (8–13). Thus, by inference, hyperconnected hubs within an individual module may be indispensable to regulation and function of the module as a whole, and we wanted to test this concept in relationship to the atopy-associated module. To identify putative atopy-associated hyperconnected hubs, we first calculated the cumulative connectivity of each gene within the atopy-associated module (i.e., intramodular connectivity (k_{in}); see *Materials and Methods*). Genes that are highly correlated with many genes in the module will have large values for k_{in}, and vice versa. The statistical reliability of the network measure k_{in} is unknown in the current experimental setting, and hence we calculated the k_{in} separately for both independent atopic data sets. As illustrated in Fig. 3*A*, the analyses demonstrated that variations in connectivity within the atopic module are highly reproducible (Spearman rho = 0.84, p value $<1 \times 10^{-15}$). Moreover, several hyperconnected hubs were identified, and these appear in the upper right region of Fig. 3*A*. To illustrate the wiring diagram of the atopy module, the pairwise interaction data (i.e., pairwise correlation data) were submitted to a bioinformatics tool for network visualization (33). As shown in Fig. 3*B*, the hubs manifest as the large nodes at the center of the network depiction, which are hyperconnected to peripheral nodes of low connectivity.

As detailed above, the initial identification of these putative atopy-associated hub genes was based solely on the strength of underlying statistical associations, and additional levels of (more direct) proof are required to determine the level of biological plausibility inherent in the information obtained via this approach. To explore this question we focused on two hub genes (IL-2R, IL-4R) in pathways whose functionality in relation to the Th2 cascade is well established (34, 35), and for which blocking reagents are readily accessible. The novelty of the new information on the allergen-triggered Th2 cascade provided via this approach (Fig. 3*B*) concerns the additional range of genes putatively "networked" with IL-2R and IL-4R in this module. In particular, if the linkages identified exist in vivo and are biologically meaningful, then blocking these hubs alone or in combination may affect the overall structural integrity of the module, including the expression of these previously unrecognized members of the cascade. To test this proposition, positive and negative perturbation experiments were performed by supplementing the PBMC cultures with exogenous recombinant IL-2 or IL-4, or relevant neutralizing Abs. At the termination of the cultures, $CD4^+$ Th cells were isolated and expression of the module was profiled by qRT-PCR. As illustrated in Fig. 4, hierarchical clustering analysis of these data segregated the genes into two distinct parallel pathways/clusters. The top cluster contained IL-4R, and genes within this cluster were highly induced by treatment with rIL-4 and strongly abrogated by anti-IL-4. In contrast, the bottom cluster contained IL-2R, and genes within this cluster were highly induced by treatment with rIL-2 and strongly abrogated by anti-IL-2. Strikingly, the combination of anti-IL-2 plus anti-IL-4 silenced expression of almost every gene in the module that was investigated (see supplemental Table S4 for detailed statistical analyses). Importantly, many genes within the module are totally novel (Table I), and thus their regulation by

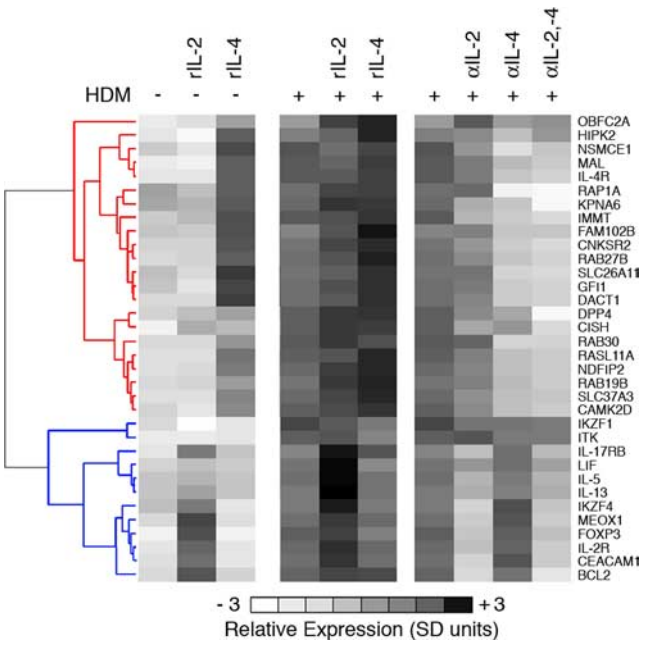

FIGURE 4. IL-2R and IL-4R are principal hubs driving the expression of the atopy-associated module. PBMC from HDM-sensitized atopics (n = 8) were cultured in the presence (+) or absence (−) of HDM, rIL-2, rIL-4, or neutralizing Abs against IL-2 (αIL-2), or IL-4 (αIL-4), or both (αIL-2,-4). At the termination of the 24-h cultures, $CD4^+$ Th cells were purified and expression of a subset of genes from the atopy-associated module was profiled by qRT-PCR. The qRT-PCR data were normalized to the stably expressed gene EEF1A1 (68), averaged across the subjects, mean centered (26), and scaled for unit variance (26). Hierarchical clustering (10) was performed on the genes to partition them into clusters of coexpressed genes. Two major expression patterns were identified that corresponded to genes that were regulated by IL-4 (red cluster dendrogram) or IL-2 (blue cluster dendrogram) genes. Detailed statistical analyses were also performed and are presented in supplemental Table S4. Additional cultures were set up with appropriate isotype control Abs, and these did not substantively affect expression profiles (not shown).

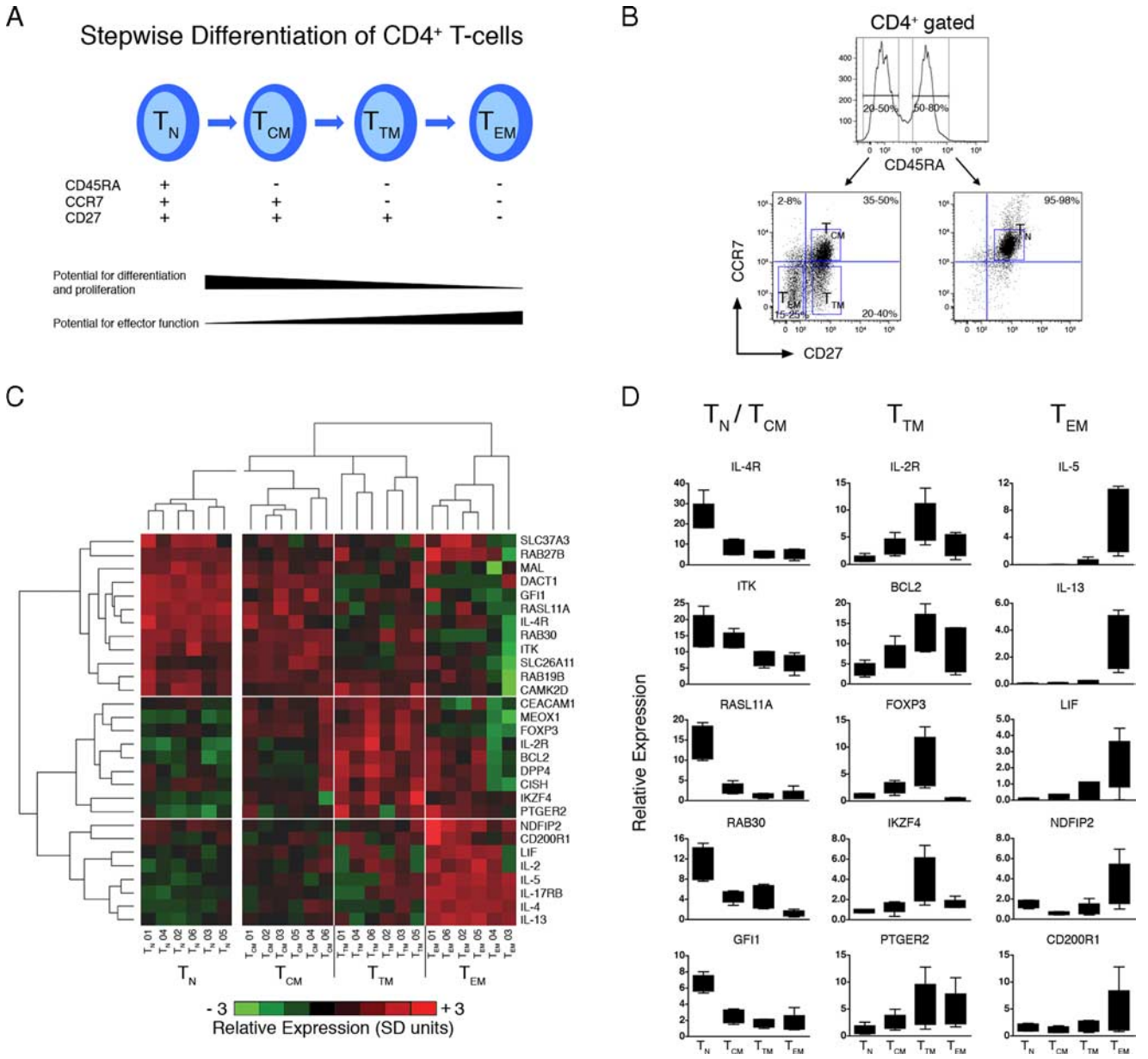

FIGURE 5. Expression of the atopy-associated module varies across naive and memory CD4$^+$ Th cell subsets. *A*, Stepwise model of CD4$^+$ Th cell memory differentiation (38). *B*, Multiparametric cell sorting strategy employed to isolate CD4$^+$ Th cell subsets. *C*, PBMC from HDM-sensitized atopics ($n = 6$) were stimulated with HDM for 20 h. At the termination of the cultures, multiparametric cell sorting was employed to isolate T_N, T_{CM}, T_{TM}, and T_{EM} subpopulations. Expression of a subset of genes from the atopy-associated module was profiled by qRT-PCR. The qRT-PCR data were normalized to the stably expressed gene EEF1A1 (68), $\log_2$ transformed, mean centered (26), and scaled for unit variance (26). Mean centering and unit variance were performed separately for the naive and memory compartments to emphasize variations across the latter compartment. Hierarchical clustering (10) was employed to identify clusters of coexpressed genes, as well as clusters of samples with similar expression profiles. Four major sample clusters and three major gene clusters were identified, as shown by the respective vertical and horizontal white lines. Detailed statistical analyses were performed and are presented in supplemental Table S5. *D*, Box-and-whisker plots of the qRT-PCR data (centering, scaling, and log transformation were not performed) for selected genes from *C*. See supplemental Table S6 for complete data set.

IL-2 and IL-4 signaling was predicted solely on the basis of their interconnectivity with IL-2R/IL-4R.

Expression of the atopy-associated module varies across the CD4$^+$ Th memory compartment

The network analyses presented above demonstrate that IL-2R and IL-4R are hyperconnected within the atopy-associated module, and that dual inhibition of these parallel pathways destabilizes gene expression programs in the overall Th memory response in a comprehensive fashion. However, it is not clear why the atopy module contains gene expression signatures associated with the early differentiation of Th2 cells (28), Th2 memory responses (16), and Treg function (30). One possibility is that because the Th memory compartment is phenotypically and functionally heterogeneous (36), the above analyses on total CD4 T cells are likely to have provided an oversimplified picture. A series of experimental observations support a relationship between the phenotype, function, and stage of CD4$^+$ Th cell memory differentiation (reviewed in Ref. 37). One simple model to account for the origin of these diverse subsets proposes that there is a stepwise differentiation of naive Th cells (T_N) $\rightarrow$ central memory (T_{CM}) $\rightarrow$ transitory memory (T_{TM}) $\rightarrow$ effector memory (T_{EM}) (Fig. 5*A*) (36, 38). To

investigate expression of the module across the differentiation pathway during a Th memory response, PBMC from six HDM-allergic subjects were stimulated with HDM for 20 h. At the termination of the cultures, $CD4^+$ Th cell subsets were isolated by multiparametric cell sorting employing the markers CD4, CD45RA, CCR7, and CD27 (Fig. 5*B*) (38), and gene expression was profiled by qRT-PCR.

As illustrated in Fig. 5*C*, analysis of the qRT-PCR data by hierarchical clustering demonstrated that expression of the module partitioned unevenly across the differentiation pathway (see supplemental Table S5 for statistical analyses). For instance, IL-4R-associated genes (e.g., DACT1, GFI1, MAL, RAB30, RASL11A, SLC26A11) were highly expressed in naive and to a lesser extent in central memory, whereas Treg-associated genes (IL-2R, FoxP3) were highly expressed in central memory relative to naive memory, but peaked together with several other genes (CEACAM1, CISH, DPP4, IKZF4) within transitory memory (Fig. 5, *C* and *D*). The effector memory compartment was characterized by high level expression of genes associated with effector functions (IL-2, IL-4, IL-5, IL-13, IL-17RB, LIF), together with the NF-κB regulator NDFIP2 and the inhibitory receptor CD200R1 (Fig. 5, *C* and *D*). These data demonstrate that naive Th cells participate in the Th memory response, and further show that the Treg and Th2-associated signatures segregate in the T_{TM} and T_{EM} compartments, respectively.

Discussion

Our findings demonstrate that the hallmark of the atopic phenotype at the systems level is the activation of an interconnected module enriched for Th2 and Treg-associated expression signatures, networked together with an additional series of 25 novel genes not previously associated with atopy. Of note, application of network analysis techniques to the microarray data not only confirmed the importance of the bulk of Th2-associated genes identified by more conventional analyses in previous studies (16, 28), but it also added a second tier of previously unrecognized Th2-associated genes identified purely on the basis of their patterns of interconnectivity with other members of the atopy module (Table I). These novel genes encode proteins mainly involved in generic functions such as transcriptional regulation and signal transduction; however, their precise function in allergen-driven Th cell responses remains to be investigated. In the parlance of this emerging field, genes in the network displaying highest overall connectivity strengths are designated as hubs, which are ascribed key roles in overall network functionality (8–13). Confirmation that the gene interconnectivity measures employed to reconstruct this atopy-associated module have a biological as opposed to purely statistical basis was provided via blocking experiments targeting the hubs IL-2R and IL-4R. Notably, disruption of IL-2 and IL-4 signaling during stimulation of Th memory cells with specific allergen collapsed the overall atopy module including expression of these novel genes. This finding justifies further pursuit of this overall approach, in particular studies related to the network regulatory functions of other "novel" hub genes. The most direct approach would be to employ small interfering RNA-mediated knockdown of hub(s), as has been performed in Th cell lines (28); however, effective methodology is not available to achieve this in primary human Th memory responses.

An alternative approach to probe further into the function of the gene network that we are following involves more precise cellular localization of relevant expression signals during the Th memory response. Recent literature indicates that reactivation of Th memory cells sets in train a stepwise differentiation process giving rise to functionally distinct memory subpopulations (36–38), and the expression signals we are detecting likely represent a summation of the activity of these subsets. We hypothesized that resolving the allergen-activated $CD4^+$ Th cell population into discrete memory subsets before expression analysis may provide some clarity to this complex picture. This approach has resulted in a series of novel observations, and in particular it has facilitated partitioning of key elements of the overall atopy module expression signal to different stages of the Th memory response. Our findings demonstrated that IL-4-associated genes were predominantly expressed at early stages of differentiation (T_N, T_{CM}), whereas IL-2-regulated genes were expressed at early (T_{CM}) and later stages (T_{TM}, T_{EM}). Moreover, we found that Treg and Th2 effector signatures partitioned into the T_{TM} and T_{EM} compartments, respectively. While we did not perform functional assays to determine whether the T_{TM} ($CD27^+$) subset had suppressive activity, CD27 has been previously reported to discriminate regulatory from effector T cells (39). Moreover, we detected a bona fide Treg signature in the T_{TM} compartment, which includes genes such as IKZF4 (Eos) that are highly specific for Tregs (30).

The nature of the relationship between Tregs and conventional T cells is a contentious issue. Several laboratories have demonstrated that expression of FoxP3 is up-regulated as a normal consequence of human CD4 T cell activation (40–42), and it has been suggested that regulatory activity may be a reversible peripheral state of differentiation (reviewed in Ref. 27). However, the interpretation of these data is confounded by the knowledge that FoxP3 expression does not necessarily confer suppressive activity (41–43). Moreover, concerns have been raised about the specificity of FoxP3 staining in activated T cells (41, 44). One possible interpretation of our data is that the T_{CM} compartment gives rise to both T_{EM} and Tregs, either via parallel or sequential pathways that are programmed by IL-2. Indeed, an IL-2-dependent mechanism drives the development of Ag-specific effector and regulatory T cells from the same naive precursors in animal models of autoimmune disease (45), and we observed that both Th2 effector and Treg-associated signatures are dependent on IL-2 (Fig. 4). Data from human studies suggest that Tregs may be derived from the allergen-driven expansion of memory T cells (46, 47). In human T cells, IL-2-driven FoxP3 expression does not bestow de novo immunoregulatory properties until at least 4 days of stimulation (42). This delayed acquisition of regulatory function provides a plausible mechanism to generate adaptive Tregs that can switch off acute inflammation, thus preventing chronic disease (45, 48, 49).

The synchronous activation of the Treg and Th2 machinery during recall responses to allergens may explain the inherent plasticity of the CD4 compartment, which has recently been documented at the epigenetic level (50). Studies in animal models have shown that in some circumstances Tregs can be converted into Th2 effectors via internal regulation of their gene expression program (43, 51). In this context it is also noteworthy that PTGER2 was highly expressed in the T_{TM} and T_{EM} compartments (supplemental Table S6), because signaling via this pathway can convert conventional T cells into Tregs via induction of FoxP3 (52, 53). Further studies are warranted to investigate this possibility in allergy.

The presence of a parallel IL-4-dependant activation signal in the naive Th cell compartment was striking. Although it has been reported that the role of IL-4 is redundant in some (54) but not all models (55) of Th2 differentiation in vivo, IL-4 is essential for the collateral priming of naive Th cells to other bystander allergens (56). Bystander sensitization is a recognized feature of persistent allergic disease in humans (reviewed in Ref. 49), and it is also noteworthy that successful allergen-specific immunotherapy against single allergens prevents sensitization to new allergens (reviewed in Ref. 57).

The identification of IL-2R as a T cell activation-associated, atopy-associated hub is intriguing. Systematic studies of disease-gene relationships across multiple disorders have suggested that common pathways may underlie susceptibility to many diseases (58), especially inflammatory diseases (59, 60). IL-2R may represent an archetypal example of a hub that is relevant to multiple inflammatory diseases, because disruption of IL-2 signaling in mice leads to autoimmunity (61). Moreover, genetic variants in IL-2R differentially confer risk to type I diabetes and multiple sclerosis in humans (62). The relevance of this pathway to the pathogenesis of human asthma was recently demonstrated in a clinical trial, where blocking IL-2R improved lung function and asthma control in patients with moderate to severe disease (63). Further studies are now warranted to determine whether genetic variation in the IL-2R locus is important in disease risk and severity.

This study has significant limitations that require addressing in follow-up investigations. In particular, for logistical reasons we focused on a single time point after Th cell activation; however, biological systems are best modeled in dynamic terms (64). Moreover, we have shown in previous kinetic studies that the 24 h time point favors identification of Th2 activation/differentiation-associated genes in contrast to late effector genes such as IFN-γ (16) and TNF-α, which also contribute to asthma pathogenesis (17). This approach also cannot reproduce microenvironmental conditions at the asthma lesional site where T cell triggering is controlled by highly differentiated mucosal dendritic cells (65). Additionally, as noted in *Results*, the focus on IL-2R and IL-4R genes was dictated by the availability of relevant inhibitors, and more systematic study of the role of other potential hubs in the Th2 network will require utilization of a wider range of blocking reagents. Such functional studies are important because unlike the situation in protein interaction networks, which are based on detection of protein-protein interactions in functional assays, coexpression networks represent more general relationships between genes that are simply based on statistical correlations and not on functional data. Thus, the biological significance of the other putative hubs is unknown in the absence of functional data. Notwithstanding these limitations, this study has provided novel insight into the operation of the Th2 cascade in human atopics, and in doing so illustrates some important principles that are readily applicable to research into a broad range of other immunoinflammatory diseases. Notably, our findings demonstrate how inferences derived from network analysis can be used to identify novel disease-associated genes within causal pathways and place them within a testable functional context. This approach thus has the potential to accelerate drug discovery programs aimed at destabilization of inflammatory gene networks rather than inhibiting individual effector molecules. The latter approach is currently the dominant paradigm in pharmacology and has shown only limited success in the treatment of allergic diseases (66, 67). Finally, network analysis may also increase capacity to identify subtle gene/gene regulatory interactions that escape detection via conventional microarray methodology, and thus may also enhance the precision of basic mechanistic studies.

Acknowledgments

We thank Matt Wikstrom, Debbie Strickland, Jenny Thomas, Rob Shackleton, and Barb Holt for help and advice regarding cell sorting and handling techniques.

Disclosures

The authors have no financial conflicts of interest.

References

1. Schadt, E. E., A. Sachs, and S. Friend. 2005. Embracing complexity, inching closer to reality. *Sci. STKE* 2005: pe40.
2. Van Regenmortel, M. H. 2004. Reductionism and complexity in molecular biology: scientists now have the tools to unravel biological and overcome the limitations of reductionism. *EMBO Rep.* 5: 1016–1020.
3. Barabasi, A. L., and Z. N. Oltvai. 2004. Network biology: understanding the cell's functional organization. *Nat. Rev. Genet.* 5: 101–113.
4. Kitano, H. 2004. Biological robustness. *Nat. Rev. Genet.* 5: 826–837.
5. Giaever, G., A. M. Chu, L. Ni, C. Connelly, L. Riles, S. Veronneau, S. Dow, A. Lucau-Danila, K. Anderson, B. Andre, et al. 2002. Functional profiling of the *Saccharomyces cerevisiae* genome. *Nature* 418: 387–391.
6. Bergman, A., and M. L. Siegal. 2003. Evolutionary capacitance as a general feature of complex gene networks. *Nature* 424: 549–552.
7. Luscombe, N. M., M. M. Babu, H. Yu, M. Snyder, S. A. Teichmann, and M. Gerstein. 2004. Genomic analysis of regulatory network dynamics reveals large topological changes. *Nature* 431: 308–312.
8. Albert, R., H. Jeong, and A. L. Barabasi. 2000. Error and attack tolerance of complex networks. *Nature* 406: 378–382.
9. Davierwala, A. P., J. Haynes, Z. Li, R. L. Brost, M. D. Robinson, L. Yu, S. Mnaimneh, H. Ding, H. Zhu, Y. Chen, et al. 2005. The synthetic genetic interaction spectrum of essential genes. *Nat. Genet.* 37: 1147–1152.
10. Carlson, M. R., B. Zhang, Z. Fang, P. S. Mischel, S. Horvath, and S. F. Nelson. 2006. Gene connectivity, function, and sequence conservation: predictions from modular yeast co-expression networks. *BMC Genomics* 7: 40.
11. Jeong, H., S. P. Mason, A. L. Barabasi, and Z. N. Oltvai. 2001. Lethality and centrality in protein networks. *Nature* 411: 41–42.
12. Lee, I., B. Lehner, C. Crombie, W. Wong, A. G. Fraser, and E. M. Marcotte. 2008. A single gene network accurately predicts phenotypic effects of gene perturbation in *Caenorhabditis elegans*. *Nat. Genet.* 40: 181–188.
13. Jeong, H., B. Tombor, R. Albert, Z. N. Oltvai, and A. L. Barabasi. 2000. The large-scale organization of metabolic networks. *Nature* 407: 651–654.
14. Yu, H., P. Braun, M. A. Yildirim, I. Lemmens, K. Venkatesan, J. Sahalie, T. Hirozane-Kishikawa, F. Gebreab, N. Li, N. Simonis, et al. 2008. High-quality binary protein interaction map of the yeast interactome network. *Science* 322: 104–110.
15. Benoist, C., R. N. Germain, and D. Mathis. 2006. A plaidoyer for "systems immunology". *Immunol. Rev.* 210: 229–234.
16. Bosco, A., K. L. McKenna, C. J. Devitt, M. J. Firth, P. D. Sly, and P. G. Holt. 2006. Identification of novel Th2-associated genes in T memory responses to allergens. *J. Immunol.* 176: 4766–4777.
17. Heaton, T., J. Rowe, S. Turner, R. C. Aalberse, N. de Klerk, D. Suriyaarachchi, M. Serralha, B. J. Holt, E. Hollams, S. Yerkovich, et al. 2005. An immunoepidemiological approach to asthma: identification of in-vitro T-cell response patterns associated with different wheezing phenotypes in children. *Lancet* 365: 142–149.
18. Smyth, G. K. 2004. Linear models and empirical Bayes methods for assessing differential expression in microarray experiments. *Stat. Appl. Genet. Mol. Biol.* 3: article 3.
19. Benjamini, Y., and Y. Hochberg. 1995. Controlling the false discovery rate: a practical and powerful approach to multiple testing. *J. R. Stat. Soc. Ser. B* 57: 289–300.
20. Tusher, V. G., R. Tibshirani, and G. Chu. 2001. Significance analysis of microarrays applied to the ionizing radiation response. *Proc. Natl. Acad. Sci. USA* 98: 5116–5121.
21. Cui, X., and G. A. Churchill. 2003. Statistical tests for differential expression in cDNA microarray experiments. *Genome Biol.* 4: 210.
22. Ravasz, E., A. L. Somera, D. A. Mongru, Z. N. Oltvai, and A. L. Barabasi. 2002. Hierarchical organization of modularity in metabolic networks. *Science* 297: 1551–1555.
23. Langfelder, P., B. Zhang, and S. Horvath. 2008. Defining clusters from a hierarchical cluster tree: the Dynamic Tree Cut library for R. *Bioinformatics* 24: 719–720.
24. Efron, B., and R. Tibshirani. 2007. On testing the significance of sets of genes. *Ann. Appl. Stat.* 1: 107–109.
25. Benjamini, Y., and D. Yekutieli. 2001. The control of the false discovery rate in multiple testing under dependency. *Ann Stat.* 29: 1165–1188.
26. van den Berg, R. A., H. C. Hoefsloot, J. A. Westerhuis, A. K. Smilde, and M. J. van der Werf. 2006. Centering, scaling, and transformations: improving the biological information content of metabolomics data. *BMC Genomics* 7: 142.
27. Pillai, V., and N. J. Karandikar. 2007. Human regulatory T cells: a unique, stable thymic subset or a reversible peripheral state of differentiation? *Immunol. Lett.* 114: 9–15.
28. Lund, R. J., M. Loytomaki, T. Naumanen, C. Dixon, Z. Chen, H. Ahlfors, S. Tuomela, J. Tahvanainen, J. Scheinin, T. Henttinen, et al. 2007. Genome-wide identification of novel genes involved in early Th1 and Th2 cell differentiation. *J. Immunol.* 178: 3648–3660.
29. Schadt, E. E., and P. Y. Lum. 2006. Thematic review series: systems biology approaches to metabolic and cardiovascular disorders: reverse engineering gene networks to identify key drivers of complex disease phenotypes. *J. Lipid Res.* 47: 2601–2613.
30. Hill, J. A., M. Feuerer, K. Tash, S. Haxhinasto, J. Perez, R. Melamed, D. Mathis, and C. Benoist. 2007. Foxp3 transcription-factor-dependent and -independent regulation of the regulatory T cell transcriptional signature. *Immunity* 27: 786–800.
31. Chaussabel, D., C. Quinn, J. Shen, P. Patel, C. Glaser, N. Baldwin, D. Stichweh, D. Blankenship, L. Li, I. Munagala, et al. 2008. A modular analysis framework

for blood genomics studies: application to systemic lupus erythematosus. *Immunity* 29: 150–164.
32. Chuaqui, R. F., R. F. Bonner, C. J. Best, J. W. Gillespie, M. J. Flaig, S. M. Hewitt, J. L. Phillips, D. B. Krizman, M. A. Tangrea, M. Ahram, et al. 2002. Post-analysis follow-up and validation of microarray experiments. *Nat. Genet.* 32(Suppl.): 509–514.
33. Hu, Z., J. Mellor, J. Wu, T. Yamada, D. Holloway, and C. Delisi. 2005. VisANT: data-integrating visual framework for biological networks and modules. *Nucleic Acids Res.* 33: W352–W357.
34. Le Gros, G., S. Z. Ben-Sasson, R. Seder, F. D. Finkelman, and W. E. Paul. 1990. Generation of interleukin 4 (IL-4)-producing cells in vivo and in vitro: IL-2 and IL-4 are required for in vitro generation of IL-4-producing cells. *J. Exp. Med.* 172: 921–929.
35. Swain, S. L., A. D. Weinberg, M. English, and G. Huston. 1990. IL-4 directs the development of Th2-like helper effectors. *J. Immunol.* 145: 3796–3806.
36. Sallusto, F., D. Lenig, R. Forster, M. Lipp, and A. Lanzavecchia. 1999. Two subsets of memory T lymphocytes with distinct homing potentials and effector functions. *Nature* 401: 708–712.
37. Harari, A., V. Dutoit, C. Cellerai, P. A. Bart, R. A. Du Pasquier, and G. Pantaleo. 2006. Functional signatures of protective antiviral T-cell immunity in human virus infections. *Immunol. Rev.* 211: 236–254.
38. Fritsch, R. D., X. Shen, G. P. Sims, K. S. Hathcock, R. J. Hodes, and P. E. Lipsky. 2005. Stepwise differentiation of CD4 memory T cells defined by expression of CCR7 and CD27. *J. Immunol.* 175: 6489–6497.
39. Ruprecht, C. R., M. Gattorno, F. Ferlito, A. Gregorio, A. Martini, A. Lanzavecchia, and F. Sallusto. 2005. Coexpression of CD25 and CD27 identifies FoxP3$^+$ regulatory T cells in inflamed synovia. *J. Exp. Med.* 201: 1793–1803.
40. Walker, M. R., D. J. Kasprowicz, V. H. Gersuk, A. Benard, M. Van Landeghen, J. H. Buckner, and S. F. Ziegler. 2003. Induction of FoxP3 and acquisition of T regulatory activity by stimulated human CD4$^+$CD25$^-$ T cells. *J. Clin. Invest.* 112: 1437–1443.
41. Tran, D. Q., H. Ramsey, and E. M. Shevach. 2007. Induction of FOXP3 expression in naive human CD4$^+$FOXP3 T cells by T-cell receptor stimulation is transforming growth factor-β dependent but does not confer a regulatory phenotype. *Blood* 110: 2983–2990.
42. Zheng, Y., C. N. Manzotti, F. Burke, L. Dussably, O. Qureshi, L. S. Walker, and D. M. Sansom. 2008. Acquisition of suppressive function by activated human CD4$^+$CD25$^-$ T cells is associated with the expression of CTLA-4 not FoxP3. *J. Immunol.* 181: 1683–1691.
43. Wan, Y. Y., and R. A. Flavell. 2007. Regulatory T-cell functions are subverted and converted owing to attenuated Foxp3 expression. *Nature* 445: 766–770.
44. Pillai, V., and N. J. Karandikar. 2008. Attack on the clones?: human FOXP3 detection by PCH101, 236A/E7, 206D, and 259D reveals 259D as the outlier with lower sensitivity. *Blood* 111: 463–464; author reply 464–466.
45. Knoechel, B., J. Lohr, E. Kahn, J. A. Bluestone, and A. K. Abbas. 2005. Sequential development of interleukin 2-dependent effector and regulatory T cells in response to endogenous systemic antigen. *J. Exp. Med.* 202: 1375–1386.
46. Vukmanovic-Stejic, M., Y. Zhang, J. E. Cook, J. M. Fletcher, A. McQuaid, J. E. Masters, M. H. Rustin, L. S. Taams, P. C. Beverley, D. C. Macallan, and A. N. Akbar. 2006. Human CD4$^+$CD25^{hi}Foxp3$^+$ regulatory T cells are derived by rapid turnover of memory populations in vivo. *J. Clin. Invest.* 116: 2423–2433.
47. Vukmanovic-Stejic, M., E. Agius, N. Booth, P. J. Dunne, K. E. Lacy, J. R. Reed, T. O. Sobande, S. Kissane, M. Salmon, M. H. Rustin, and A. N. Akbar. 2008. The kinetics of CD4$^+$Foxp3$^+$ T cell accumulation during a human cutaneous antigen-specific memory response in vivo. *J. Clin. Invest.* 118: 3639–3650.
48. Strickland, D. H., P. A. Stumbles, G. R. Zosky, L. S. Subrata, J. A. Thomas, D. J. Turner, P. D. Sly, and P. G. Holt. 2006. Reversal of airway hyperresponsiveness by induction of airway mucosal CD4$^+$CD25$^+$ regulatory T cells. *J. Exp. Med.* 203: 2649–2660.
49. Curotto de Lafaille, M. A., N. Kutchukhidze, S. Shen, Y. Ding, H. Yee, and J. J. Lafaille. 2008. Adaptive Foxp3$^+$ regulatory T cell-dependent and -independent control of allergic inflammation. *Immunity* 29: 114–126.
50. Wei, G., L. Wei, J. Zhu, C. Zang, J. Hu-Li, Z. Yao, K. Cui, Y. Kanno, T. Y. Roh, W. T. Watford, et al. 2009. Global mapping of H3K4me3 and H3K27me3 reveals specificity and plasticity in lineage fate determination of differentiating CD4$^+$ T cells. *Immunity* 30: 155–167.
51. Joetham, A., S. Matsubara, M. Okamoto, K. Takeda, N. Miyahara, A. Dakhama, and E. W. Gelfand. 2008. Plasticity of regulatory T cells: subversion of suppressive function and conversion to enhancement of lung allergic responses. *J. Immunol.* 180: 7117–7124.
52. Baratelli, F., Y. Lin, L. Zhu, S. C. Yang, N. Heuze-Vourc'h, G. Zeng, K. Reckamp, M. Dohadwala, S. Sharma, and S. M. Dubinett. 2005. Prostaglandin E_2 induces FOXP3 gene expression and T regulatory cell function in human CD4$^+$ T cells. *J. Immunol.* 175: 1483–1490.
53. Sharma, S., S. C. Yang, L. Zhu, K. Reckamp, B. Gardner, F. Baratelli, M. Huang, R. K. Batra, and S. M. Dubinett. 2005. Tumor cyclooxygenase-2/prostaglandin E_2-dependent promotion of FOXP3 expression and CD4$^+$CD25$^+$ T regulatory cell activities in lung cancer. *Cancer Res.* 65: 5211–5220.
54. van Panhuys, N., S. C. Tang, M. Prout, M. Camberis, D. Scarlett, J. Roberts, J. Hu-Li, W. E. Paul, and G. Le Gros. 2008. In vivo studies fail to reveal a role for IL-4 or STAT6 signaling in Th2 lymphocyte differentiation. *Proc. Natl. Acad. Sci. USA* 105: 12423–12428.
55. Sokol, C. L., G. M. Barton, A. G. Farr, and R. Medzhitov. 2008. A mechanism for the initiation of allergen-induced T helper type 2 responses. *Nat. Immunol.* 9: 310–318.
56. Eisenbarth, S. C., A. Zhadkevich, P. Ranney, C. A. Herrick, and K. Bottomly. 2004. IL-4-dependent Th2 collateral priming to inhaled antigens independent of Toll-like receptor 4 and myeloid differentiation factor 88. *J. Immunol.* 172: 4527–4534.
57. Holgate, S. T., and R. Polosa. 2008. Treatment strategies for allergy and asthma. *Nat. Rev. Immunol.* 8: 218–230.
58. Goh, K. I., M. E. Cusick, D. Valle, B. Childs, M. Vidal, and A. L. Barabasi. 2007. The human disease network. *Proc. Natl. Acad. Sci. USA* 104: 8685–8690.
59. Becker, K. G., R. M. Simon, J. E. Bailey-Wilson, B. Freidlin, W. E. Biddison, H. F. McFarland, and J. M. Trent. 1998. Clustering of non-major histocompatibility complex susceptibility candidate loci in human autoimmune diseases. *Proc. Natl. Acad. Sci. USA* 95: 9979–9984.
60. Yamada, R., and K. Ymamoto. 2005. Recent findings on genes associated with inflammatory disease. *Mutat. Res.* 573: 136–151.
61. Willerford, D. M., J. Chen, J. A. Ferry, L. Davidson, A. Ma, and F. W. Alt. 1995. Interleukin-2 receptor alpha chain regulates the size and content of the peripheral lymphoid compartment. *Immunity* 3: 521–530.
62. Maier, L. M., C. E. Lowe, J. Cooper, K. Downes, D. E. Anderson, C. Severson, P. M. Clark, B. Healy, N. Walker, C. Aubin, et al. 2009. IL2RA genetic heterogeneity in multiple sclerosis and type 1 diabetes susceptibility and soluble interleukin-2 receptor production. *PLoS Genet.* 5: e1000322.
63. Busse, W. W., E. Israel, H. S. Nelson, J. W. Baker, B. L. Charous, D. Y. Young, V. Vexler, and R. S. Shames. 2008. Daclizumab improves asthma control in patients with moderate to severe persistent asthma: a randomized, controlled trial. *Am. J. Respir. Crit. Care Med.* 178: 1002–1008.
64. Kitano, H. 2002. Systems biology: a brief overview. *Science* 295: 1662–1664.
65. Holt, P. G., D. H. Strickland, M. E. Wikstrom, and F. L. Jahnsen. 2008. Regulation of immunological homeostasis in the respiratory tract. *Nat. Rev. Immunol.* 8: 142–152.
66. Hopkins, A. L. 2008. Network pharmacology: the next paradigm in drug discovery. *Nat. Chem. Biol.* 4: 682–690.
67. Kay, A. 2006. The role of T lymphocytes in asthma. *Chem. Immunol. Allergy* 91: 59–75.
68. Hamalainen, H. K., J. C. Tubman, S. Vikman, T. Kyrola, E. Ylikoski, J. A. Warrington, and R. Lahesmaa. 2001. Identification and validation of endogenous reference genes for expression profiling of T helper cell differentiation by quantitative real-time RT-PCR. *Anal. Biochem.* 299: 63–70.